Cellular Signalling 53 (2019) 246–255

Contents lists available at ScienceDirect

Cellular Signalling

journal homepage: www.elsevier.com/locate/cellsig

Microtubule destabilization caused by particulate matter contributes to lung endothelial barrier dysfunction and inflammation

Pratap Karki[a], Angelo Meliton[b], Albert Sitikov[b], Yufeng Tian[b], Tomomi Ohmura[b], Anna A. Birukova[a,b,*]

[a] Department of Medicine, University of Maryland School of Medicine, Baltimore, MD 21201, United States
[b] Section of Pulmonary and Critical Care Medicine, Department of Medicine, University of Chicago, Chicago, IL 60637, United States

ARTICLE INFO

Keywords:
Particulate matter
Vascular permeability
Lung
Endothelium
Microtubules
HDAC6

ABSTRACT

Exposure to particulate matter (PM) associated with air pollution remains a major public health concern, as it has been linked to significant increase in cardiopulmonary morbidity and mortality. Lung endothelial cell (EC) dysfunction is one of the hallmarks of cardiovascular events of lung exposure to PM. However, the role of PM in acute lung injury (ALI) exacerbation and delayed recovery remains incompletely understood. This study tested a hypothesis that PM augments lung injury and EC barrier dysfunction via microtubule-dependent mechanisms. Our data demonstrate that in pulmonary EC PM caused time- and dose-dependent remodeling of actin cytoskeleton and considerable destabilization of the microtubule (MT) network. These events led to the weakening of cell junctions and formation of actin stress fibers, resulting in disruption of lung EC monolayer and increased permeability. PM also caused ROS-dependent activation of MT-specific deacetylase, HDAC6. Suppression of HDAC6 activity by pharmacological inhibitors or siRNA-based depletion of HDAC6 abolished PM-induced EC permeability increase, which was accompanied by reduced activation of stress kinase signaling, inhibition of Rho cascade, decreased IL-6 production and suppressed activation of its downstream target STAT3. Pretreatment of pulmonary EC with IL-6 inhibitor led to inhibition of STAT3 activity and decreased PM-induced hyper-permeability. Because one of the major activators of Rho-GTPase, GEF−H1, is localized on the MT, we examined its involvement in PM-caused EC barrier compromise. Inhibition of GEF-H1 activation significantly attenuated PM-induced permeability increase. Moreover, combined inhibition of IL-6 and GEF-H1 signaling exhibited additive protective effect. Taken together, these results demonstrate a critical involvement of MT-associated signaling in the PM-induced exacerbation of lung EC barrier compromise and inflammatory response.

1. Introduction

Particulate matter (PM) air pollution has now been well recognized as a major global environmental health concern which contributes to 3.3 million premature deaths per year worldwide [1]. Multiple epidemiological studies have established that exposure to PM is a trigger for many cardiovascular and respiratory disorders such as ischemic heart disease, chronic obstructive pulmonary disease, acute lower respiratory illness and lung cancer [2–4]. In regards to the mechanisms of PM-induced cardiopulmonary pathologies, the studies have shown that PM accelerates inflammation-mediated thrombosis [5–7]. PM-induced mitochondrial reactive oxygen species (ROS) release plays a critical role in the development of these pathological cascades [8,9]. Moreover, PM may also alter the expression of inflammatory molecules through complex pathways including DNA methylation-mediated epigenetic modification and changes in microRNAs expression [10–12].

Both in vitro as well as in vivo findings have provided evidence that PM induces lung injury and inflammation via endothelial dysfunction [13–15]. Endothelial cells (EC) are the key components of lung barrier and any compromise to EC barrier integrity leads to vascular leak and inflammation. It has long been suggested that EC could be the target of PM exposure, but underlying mechanisms of PM-induced EC

Non-standard abbreviations: EC, Endothelial cells; GEF-H1, Guanine nucleotide exchange factor H1; HDAC6, Histone deacetylase 6.; HPAEC, Human pulmonary artery endothelial cells; MT, Microtubules; nsRNA, Non-specific RNA; PM, Particulate matter; ROS, Reactive oxygen species; TER, Transendothelial electrical resistance; TubA, Tubastatin A; XPerT, Express permeability testing assay

* Corresponding address at: Department of Medicine, UMSOM Lung Biology Program, University of Maryland School of Medicine, 20 Penn Street, HSF-2, Room S143, Baltimore, MD 21201, United States.
E-mail address: abirukova@som.umaryland.edu (A.A. Birukova).

https://doi.org/10.1016/j.cellsig.2018.10.010
Received 17 May 2018; Received in revised form 15 October 2018; Accepted 15 October 2018
Available online 16 October 2018
0898-6568/ © 2018 Elsevier Inc. All rights reserved.

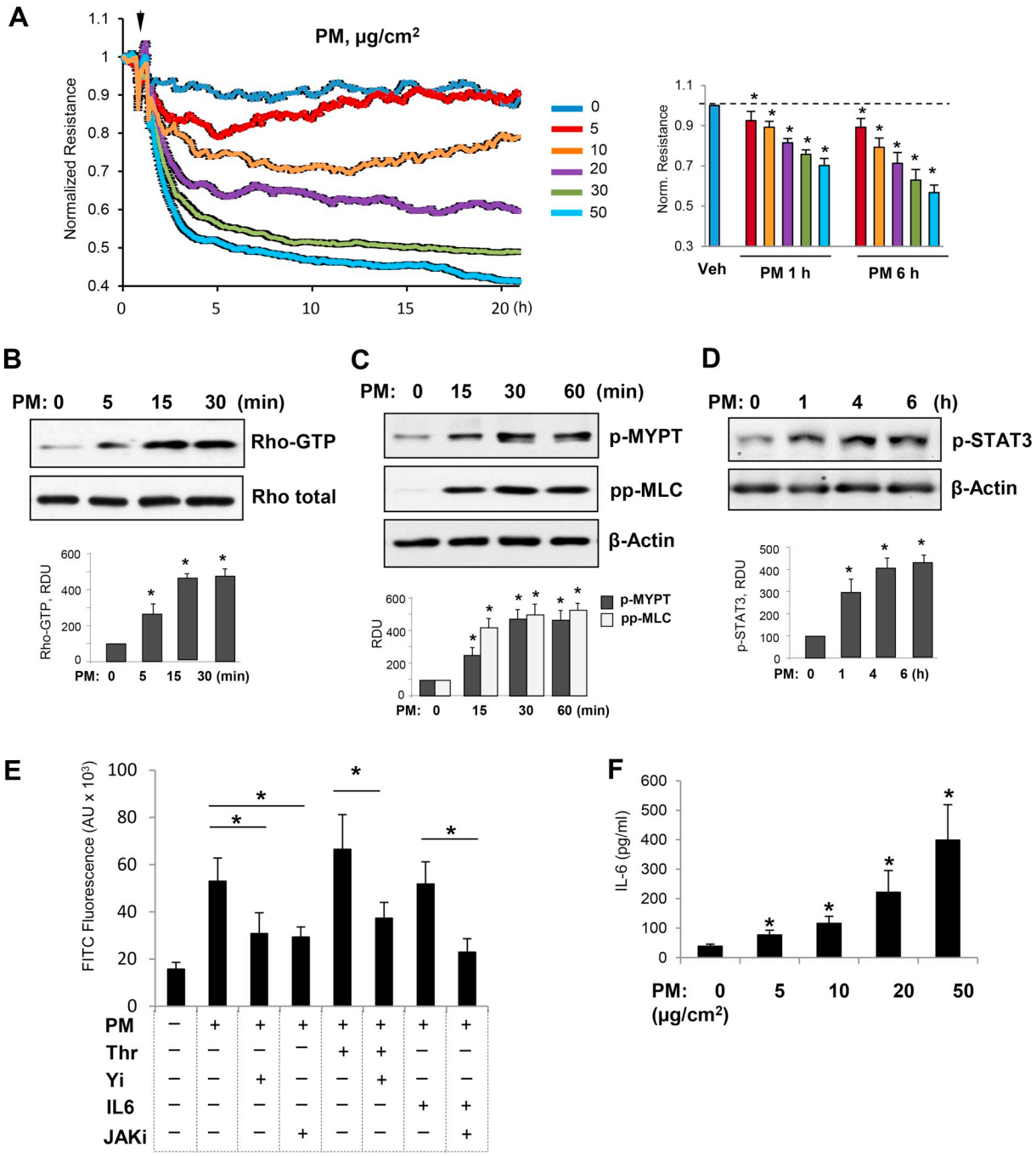

Fig. 1. PM induces EC barrier disruption by activation of Rho and IL-6 production. A - HPAEC monolayers were treated with indicated concentrations of PM (5–50 μg/cm2) and transendothelial resistance across the monolayers was measured over time. Bar graph depicts comparative measurements of TER performed in EC monolayers stimulated with various PM doses after 1 h and 6 h of treatment; n = 5; *p < 0.05. Data are expressed as mean ± SD. B - PM-treated (20 μg/cm2) EC were subjected to Rho-GTP pulldown assay using Rhotekin beads. The total Rho protein in cell lysates was used as a normalization control. The levels of: C - phospho-MYPT1, phospho-MLC; and D - phospho-STAT3 were detected by Western blotting with corresponding antibodies. Bar graphs depict quantitative densitometry analysis of western blot experiments; n = 5; **p < 0.05. Data are expressed as mean ± SD. E - Cells seeded on 96-well plates coated with biotinylated gelatin were pre-treated with JAK inhibitor (5 μM) or Rho inhibitor Y27632 (2 μM) for 30 min followed by treatment with PM (20 μg/cm^2) or IL-6/IL-6 soluble receptor (20/40 ng/mL) for 6 h and Thrombin (0.2 U/mL) for 10 min. At the end, FITC-avidin (25 μg/mL) was added for 3 min, unbound FITC-avidin was washed out, and FITC fluorescence was determined; n = 4, *p < 0.05. Data are expressed as mean ± SD. F - The levels of IL-6 in the conditioned medium were determined by ELISA after 6 h of exposure to PM. Normalized data are presented as mean ± SD; n = 4, *p < 0.05.

dysfunction are less understood. Nevertheless, IL-6 and Rho-mediated disruption of EC barrier function by PM has been reported [16,17].

In the recent years, microtubules (MT) have been identified as key regulators of endothelial permeability, but the role of MT in PM-caused EC permeability remains virtually unknown. MT cytoskeleton plays a critical role in the control of cell division and intracellular trafficking of organelles and proteins. Increasing evidences suggest that MT also play an active role in the regulation of endothelial permeability via cross-talk with actin cytoskeleton [18,19]. MT cycle between polymerized and depolymerized states and this dynamics is controlled by post-translational modifications of tubulin such as acetylation of tubulin, which confers MT stability [20,21]. A growing body of evidence

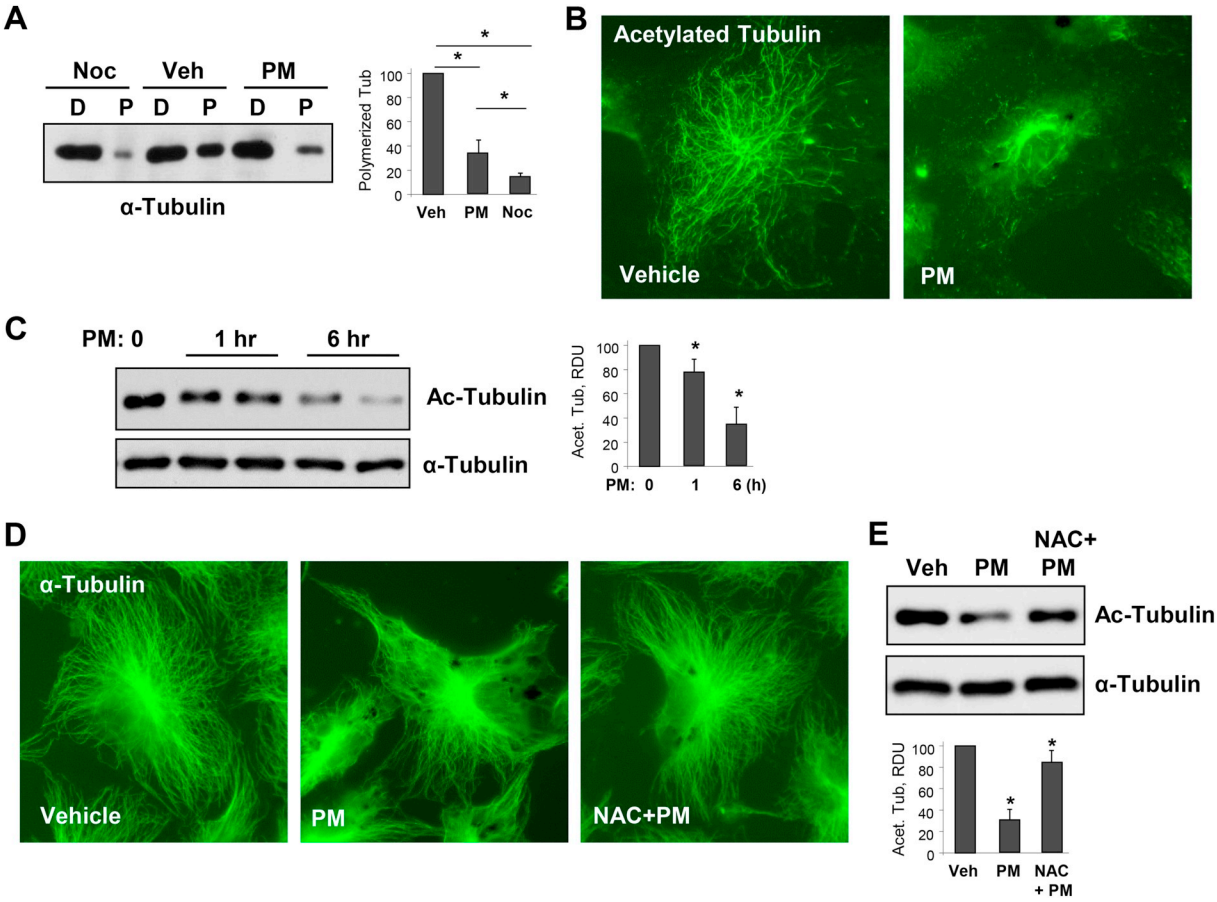

Fig. 2. PM causes MT destabilization. A - Cells were treated with vehicle, PM (20 μg/cm^2 6 h), or MT destabilizing agent nocodazole (Noc, 0.5 μM, 30 min) and MT fractionation was performed as described in Methods. Equal total protein amounts from both soluble (depolymerized, D) and pellet (polymerized, P) cellular fractions were run for Western blotting to detect α-tubulin. Bar graphs depict quantitative densitometry analysis of polymerized α-tubulin bands in western blot experiments; n = 5; **p < 0.05. Data are expressed as mean ± SD. B - HPAECs were treated with vehicle or PM (20 μg/cm^2, 6 h). The cells were then subjected for immunofluorescence staining with antibody to acetylated tubulin. Results are representative of three independent experiments. C - Cells were treated with 20 μg/cm^2 of PM for 1 h or 6 h, and cell lysates were analyzed by Western blotting to detect acetylated α-tubulin. Probing for total α-tubulin was used as a normalization control. Bar graphs depict quantitative densitometry analysis of western blot experiments; n = 3; **p < 0.05. Data are expressed as mean ± SD. D - HPAECs were pretreated with vehicle or N-acetyl cysteine (NAC, 1 mM, 30 min) followed by stimulation with vehicle or PM (20 μg/cm^2, 6 h). The cells were then subjected for immunofluorescence staining with α-tubulin antibody. Results are representative of three independent experiments. E - Cells pretreated with vehicle or NAC (1 mM, 30 min) were challenged with PM (20 μg/cm^2, 6 h) and acetylated α-tubulin was analyzed by Western blotting with acetylated α-tubulin antibody. Probing for total α-tubulin was used as a normalization control. Bar graphs depict quantitative densitometry analysis of western blot experiments; n = 3; **p < 0.05. Data are expressed as mean ± SD.

suggests that MT destabilization induced by various agonists impairs endothelial function by the activation of Rho pathway [22–27]. Furthermore, tubulin deacetylation by histone deacetylase 6 (HDAC6) is described as an essential mechanism of MT destabilization [28]. HDACs are a group of enzymes that deacetylate lysine residues from histones as well as non-histones proteins and HDAC6 falls under class IIb which is primarily localized in cytosol, where it deacetylates tubulin within the MT structures leading to MT destabilization [29,30].

In this study, we sought to determine the role of MT-associated signaling pathway in mediating PM-induced endothelial dysfunction. More precisely, we tested the hypothesis that oxidant stress-caused MT destabilization via upregulation of HDAC6 activity leads to MT destabilization accompanied by Rho-GTPase activation that ultimately results in endothelial permeability and inflammation.

2. Materials and methods

2.1. Cell culture and reagents

Human pulmonary artery endothelial cells (HPAECs) were obtained from Lonza (Allendale, NJ) and used at passages 5–8. All experiments were performed in EGM growth medium (Lonza) containing 2% fetal bovine serum unless otherwise specified. Antibodies to β-actin, α and acetylated tubulin were purchased from Sigma (St. Louis, MO); diphospho-MLC, phospho-STAT3, NFκB, HDAC6, GEF-H1 and HRP-linked anti-mouse and anti-rabbit IgG antibodies were from Cell Signaling (Beverly, MA). N-acetyl cysteine was from Sigma (St. Louis, MO). Texas Red phalloidin and Alexa Flour 488 conjugated secondary antibodies were obtained from Molecular Probes (Eugene, OR). JAK inhibitor I (Cat# 420099), Rho kinase inhibitor Y-27632 (Cat# 688000) and Tubastatin A (Cat# 382187) were received from EMD Millipore (Billerica, MA). All other biochemical reagents were from Sigma unless otherwise specified. Particulate matter: we used an urban PM collected from ambient air in Washington, DC (National Institute of Standards and Technology standard reference material, SRM 1649b). The characteristics of PM have been described by National Institute of Standards and Technology. (SRM 1649b: Urban Dust/Organics. US Department of Commerce: https://www-s.nist.gov/srmors/view_detail.cfm?srm=1649B). The product is stable at normal temperatures and pressure. Certificate Date: 12/17/2015. Expiration Date: 7/31/2030.

2.2. Measurements of transendothelial electrical resistance

The cellular barrier properties were analyzed by measurements of transendothelial electrical resistance (TER) across confluent human pulmonary endothelial monolayers grown on gold electrodes using an electrical cell-substrate impedance sensing system (Applied Biophysics, Troy, NY) as previously described [27].

2.3. EC permeability assay for macromolecules

Endothelial permeability to macromolecules was monitored by express permeability testing assay (XPerT) developed by our group [31] and now available from Millipore (Vascular Permeability Imaging Assay, cat. 17–10,398). The quantitative XPerT assay was performed in 96-well plates by measuring the fluorescence intensity of FITC in Victor X5 plate reader (PerkinElmer Life Sciences).

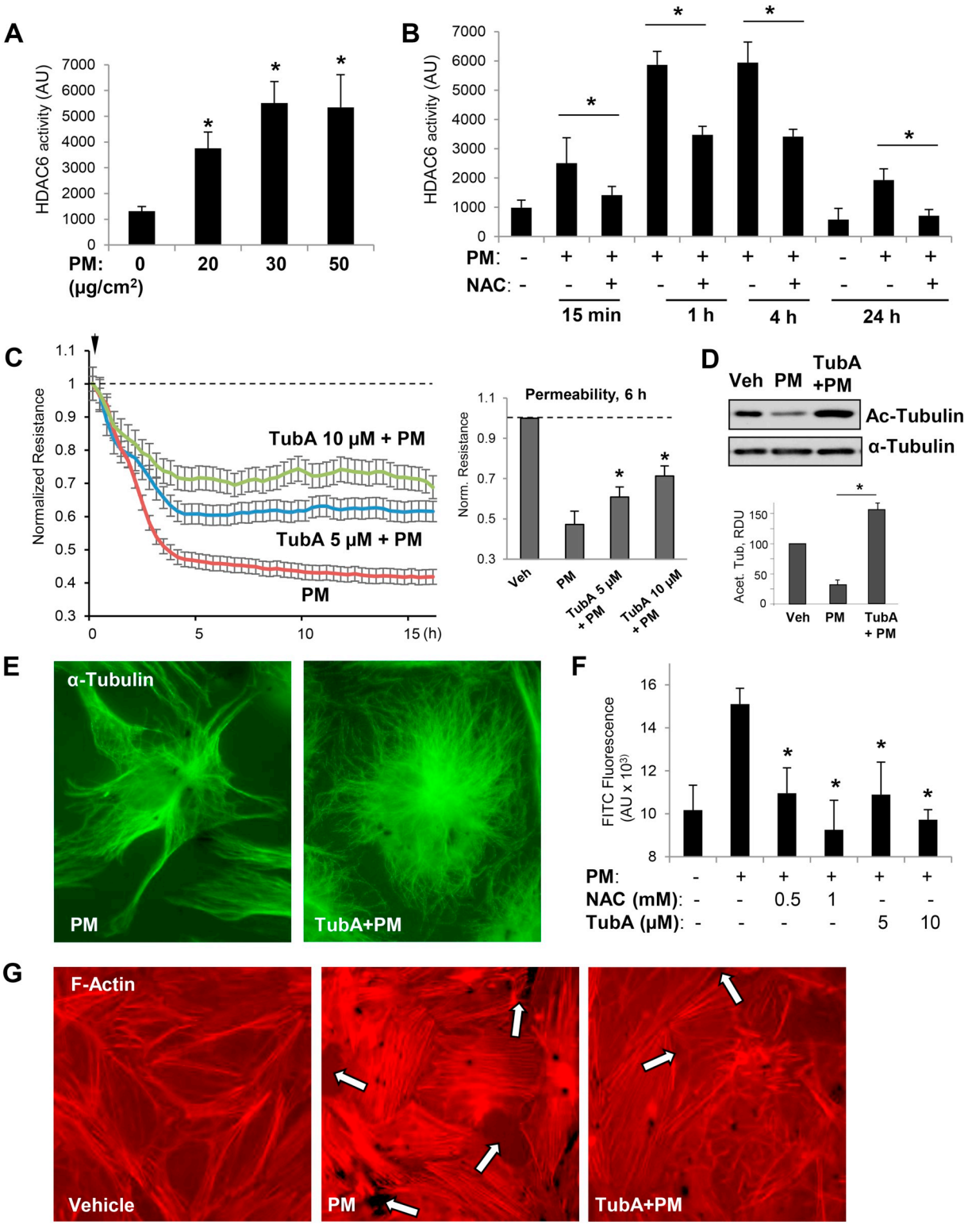

(caption on next page)

Fig. 3. PM-induced EC barrier disruption is mediated via HDAC6 activation. Cells were treated with indicated concentrations of PM (A) or stimulated with 20 μg/cm^2 PM with or without NAC (1 mM, 30 min) pretreatment for indicated periods of time (B), and HDAC6 activity assay was carried out as described in Methods; n = 3, *p < 0.05. C - TER was monitored across HPAECs monolayers challenged with PM in the presence or absence of HDAC6 inhibitor, Tubastatin (TubA, 5 μM or 10 μM). Bar graph depicts TER measurements performed in EC monolayers stimulated with PM with and without TubA pretreatment after 6 h of PM exposure; n = 3; *p < 0.05. Data are expressed as mean ± SD. D - Cell lysates prepared from EC exposed to PM (6 h) with or without TubA pretreatment were analyzed by Western blotting with acetylated α-tubulin antibody. Bar graphs depict quantitative densitometry analysis of western blot experiments; n = 3; **p < 0.05. Data are expressed as mean ± SD. E - Immunofluorescence analysis of microtubule cytoskeleton in EC exposed to PM with or without TubA pretreatment was performed using α-tubulin antibody. Results are representative of three independent experiments. F - Cells seeded on biotinylated gelatin-coated plates were pretreated with NAC (0.5, 1 mM) or TubA (5, 10 μM) for 30 min followed by PM challenge for 6 h. After incubation with FITC-avidin for 3 min, excess FITC was washed and fluorescence intensity of immobilized FITC-avidin was analyzed using microplate reader; n = 5, *p < 0.05. G - Pulmonary EC with or without TubA pretreatment (10 μM, 30 min) were stimulated with PM (20 μg/cm^2, 6 h) and subjected for immunofluorescence staining to visualize F-actin with Texas Red phalloidin. Paracellular gaps are marked by arrows. Results are representative of three independent experiments. (For interpretation of the references to colour in this figure legend, the reader is referred to the web version of this article.)

2.4. Immunofluorescent staining and image analysis

Following agonist stimulation, EC were fixed in 3.7% formaldehyde solution and permeabilized with 0.1% Triton X-100 in PBS. Incubation with antibody of interest was performed in blocking solution (2% BSA in PBS) for 1 h at room temperature followed by staining with Alexa 488-conjugated secondary antibodies. Actin filaments were stained with Texas Red-conjugated phalloidin. After immunostaining, the images were captured using an inverted microscope Nikon Eclipse TE300 connected to SPOT RT monochrome digital camera and image processor (Diagnostic Instruments, Sterling Heights, MI). The images were processed with Adobe Photoshop 7.0 (Adobe Systems, San Jose, CA).

2.5. siRNA transfections

Pre-designed HDAC6 and GEF-H1 siRNAs were purchased from Ambion (Austin, TX) and transfection in EC was done as described previously [32]. Non-specific RNA (Dharmacon, Lafayette, CO) was used as a control. Cells were used for experiments after 72 h post-transfection or harvested for western blot verification of specific protein depletion.

2.6. Immunoblotting

At the end of agonist stimulation, cells were and lysed with cold TBS-NP40 lysis buffer (20 mM Tris pH 7.4, 150 mM NaCl, 1% NP40) supplemented with protease and phosphatase inhibitor cocktails (Roche, Indianapolis, IN). Cell lysates were separated by SDS-PAGE, transferred to polyvinylidene fluoride (PVDF) membrane, and probed with specific antibodies. Equal protein loading was verified by re-probing membranes with antibody to β-actin, α-tubulin or specific protein of interest. The membranes were developed using an enhanced chemiluminescence substrate (Thermo Fisher, Waltham, MA).

2.7. MT fractionation assay

MT-enriched fractions were isolated as previously described [27]. After agonist stimulation, cells were incubated with extraction buffer containing PEM (100 mM Pipes pH 6.75, 1 mM EGTA, 1 mM MgSO4), 0.5% NP-40, protease and phosphatase inhibitor cocktail for 10 min at room temperature. The cytosolic fraction containing soluble tubulin was collected at room temperature by centrifugation at 12000 rpm for 15 min. The attached cells containing polymerized MT were collected and used for analysis of MT pool. Equal amounts of the soluble cytosolic fractions (free tubulin, depolymerized MT) and insoluble pellet (polymerized MT) were run on SDS-PAGE and probed with α-Tubulin.

2.8. Rho and GEF-H1 pulldown assays

The active RhoA and GEF-H1 were affinity precipitated from the cell lysates using purified Rhotekin and RhoA mutant (G17A) beads, respectively. The amount of activated RhoA and GEF-H1 were quantified after normalizing to total respective proteins.

2.9. Measurement of HDAC activity

HDAC6 activity was determined using a fluorogenic HDAC6 assay kit available from BPS Bioscience (San Diego, CA) following the manufacturer's instructions. Briefly, cell lysates diluted in assay buffer were mixed with the substrate followed by the addition of developer and measurement of the fluorescence values in a spectrofluorometer at excitation 380 nm and emission 460 nm.

2.10. Measurement of IL-6

IL-6 levels in conditioned medium from control and stimulated pulmonary EC were determined by ELISA (R&D Systems, Minneapolis, MN) following manufacturer's protocol. Absorbance was read at 450 nm within 30 min in microplate reader (Thermomax; Molecular Devices, Menlo Park, CA).

2.11. Statistical analysis

Results are expressed as means ± SD of three to five independent experiments. Stimulated samples were compared with controls by unpaired Student's *t*-test. For multiple-group comparisons, one-way analysis of variance (ANOVA) followed by the post hoc Fisher's test were used. $P < 0.05$ was considered statistically significant.

3. Results

Multiple signaling pathways are involved in mediating barrier disruptive effects of PM on pulmonary vascular EC. First, we examined whether PM causes EC barrier disruption in our experimental settings. On measuring TER values, our results showed that PM induces dose-dependent permeability increase in HPAECs in the 5–50 μg/cm^2 PM treatment range (Fig. 1A).The extensive studies have now established that activation of Rho is the central pathway to mediate barrier disruptive effects of various agonists [33]. Thus, we tested whether PM-induced EC barrier disruption involves activation of the Rho pathway. The results demonstrate that PM robustly activates Rho within 5–30 min after PM addition (Fig. 1B). Rho activates its downstream effector Rho-associated kinase (ROCK), which increases the levels of phosphorylated myosin light chain (MLC) either by direct phosphorylation of MLC or by phosphorylation of myosin phosphatase (MYPT) leading to suppression of MYPT enzymatic activity, ultimately leading to the actomyosin contraction, stress fiber formation, and EC dysfunction [34]. In agreement with this notion, exposure of pulmonary EC to PM increased the levels of phospho-MYPT and phospho-MCL (Fig. 1C). These results are also consistent with a recent study which showed Rho-dependent disruption of EC barrier by PM [16].

Since earlier studies have suggested that endothelial dysfunction in PM-induced disorders is accompanied by inflammation [13–15], we

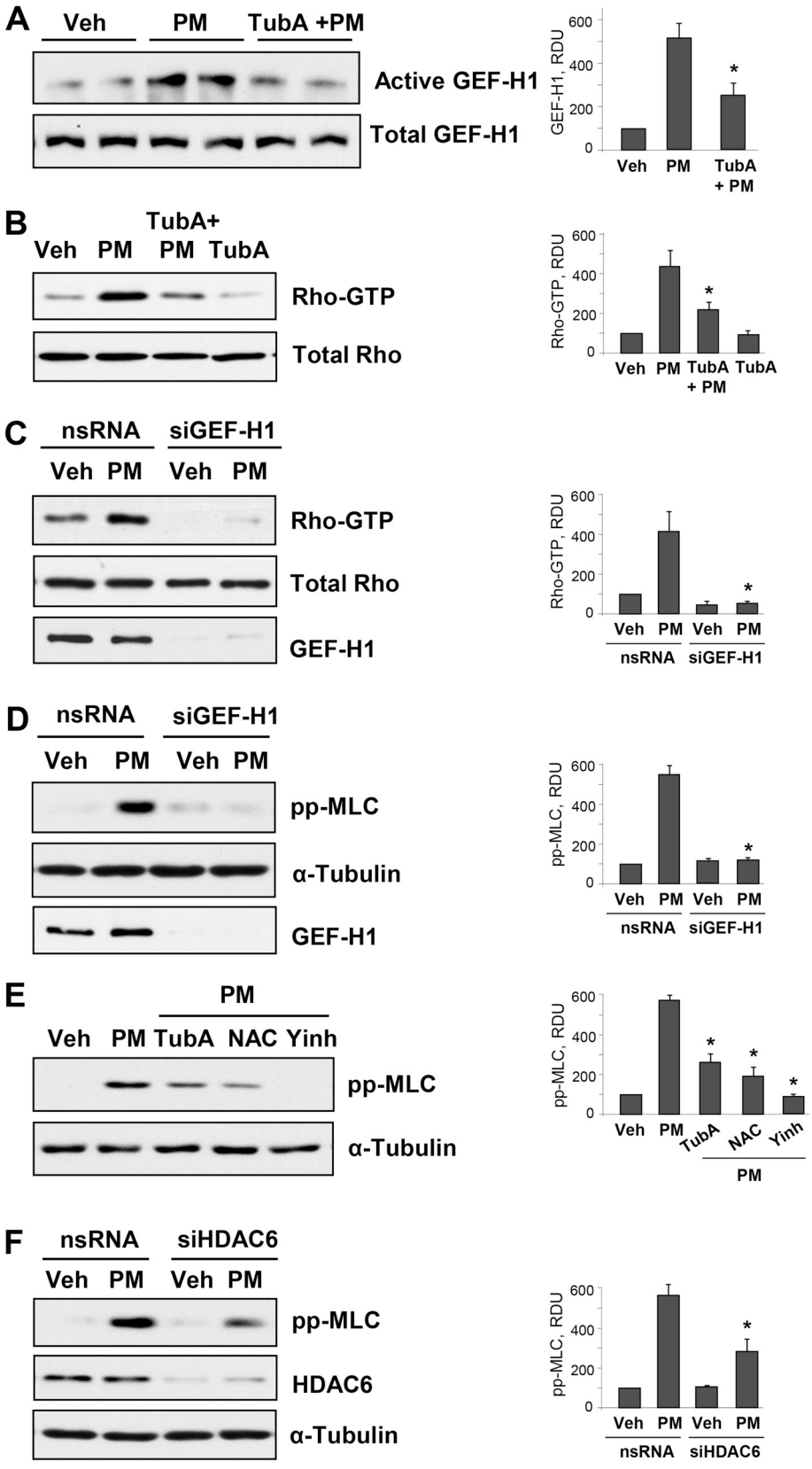

Fig. 4. Inhibition of HDAC6 attenuates PM-induced MT destabilization and Rho activation. Cells were pretreated with 10 μM of TubA for 30 min followed by PM stimulation (20 μg/cm^2, 15 min). A - GEF-H1 pulldown assay was performed to capture active GEF-H1 with immobilized RhoG17A protein beads. B - Rho-GTP pulldown assay was performed using Rhotekin beads. Total GEF-H1 and Rho proteins in respective groups were used as normalization controls. C - Rho-GTP pulldown assay of pulmonary EC transfected with non-specific (nsRNA) or GEF-H1-specific siRNA (siGEF-H1) and stimulated with PM (20 μg/cm^2, 15 min). D - Western blot analysis of phospho-MLC levels. Cells were treated as above. Efficiency of GEF-H1 knockdown was confirmed by western blot with GEF-H1 antibody. Western blot analysis of RhoA in total cell lysates and membrane reprobing for α-tubulin was used as normalization controls. E - Cells were pretreated with HDAC6 inhibitor TubA (10 μM), Rho kinase inhibitor Y27632 (2 μM) or ROS inhibitor NAC (1 mM) for 30 min followed by PM challenge (20 μg/cm^2, 6 h) and analysis of MLC phosphorylation by Western blot. F - Cells were transfected with non-specific or siRNA specific to HDAC6 (siHDAC6) followed by stimulation with PM (20 μg/cm^2, 6 h). Phospho-MLC levels were detected in cell lysates by Western blot with phospho-MLC antibody. Membrane reprobing with α-tubulin and HDAC6 antibodies was performed to verify equal loading and HDAC6 knockdown, respectively. Corresponding bar graphs depict quantitative densitometry analysis of western blot experiments; n = 3; **p < 0.05. Data are expressed as mean ± SD.

next investigated the interrelationships between inflammatory signaling and increased permeability in the PM-treated pulmonary ECs. The Janus Kinase (JAK)-mediated phosphorylation and activation of signal transducer and activator of transcription 3 (STAT3) in response to various cytokines including IL-6 plays an important role in lung inflammation [35,36]. Our results show that PM exposure induced phosphorylation of JAK substrate, STAT3, as early as 1 h and persisted for at least 6 h (Fig. 1D). To further evaluate a role of contractile and inflammatory signaling pathways in PM-induced EC permeability, we performed quantitative permeability assay to test effects of

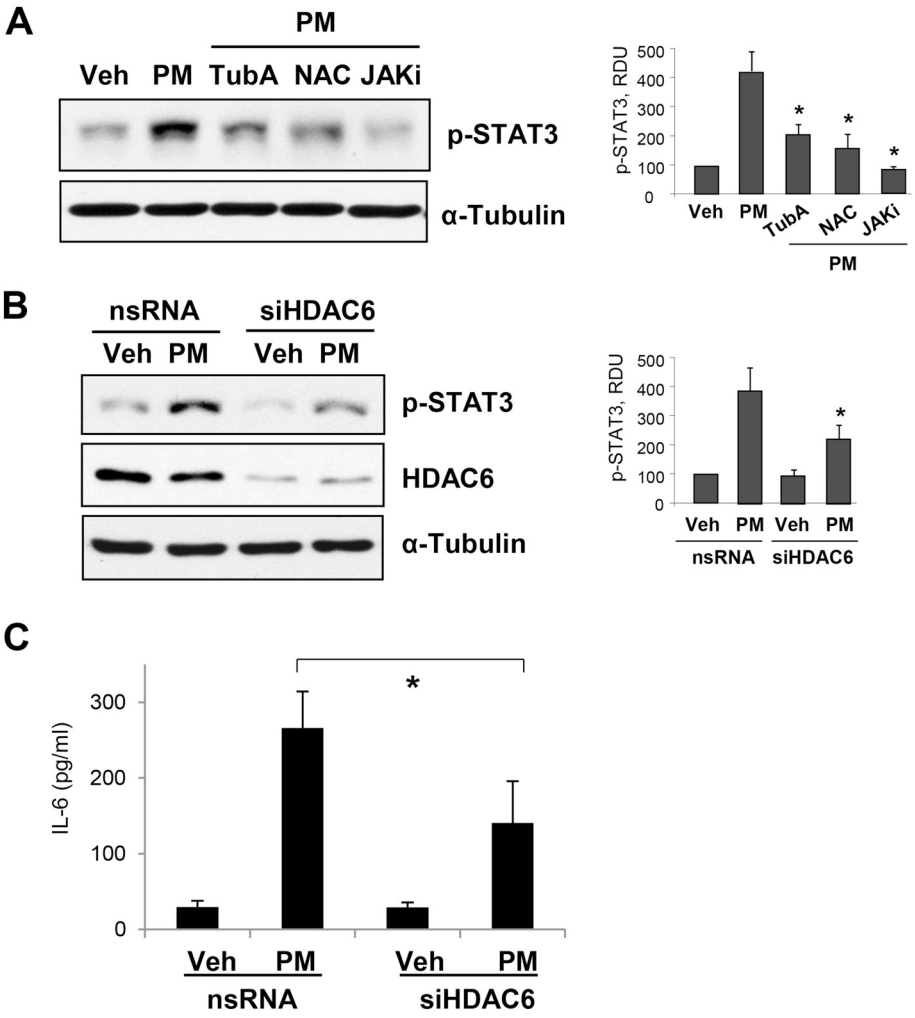

Fig. 5. HDAC6 inhibition suppresses PM-induced IL-6 increase and STAT3 activation. A - Human pulmonary EC were pre-treated with HDAC6 inhibitor TubA (10 μM), JAK inhibitor I (5 μM) or Rho inhibitor Y27632 (2 μM) for 30 min followed by treatment with PM (20 μg/cm^2, 1 h). Western blot assay using phospho-STAT3 antibody was performed to detect phospho-STAT3 levels. B - Cells transfected with non-specific or HDAC6-specific siRNA were stimulated with PM (20 μg/cm^2, 1 h), and phospho-STAT3 levels were evaluated by western blot assay was performed to determine phospho-STAT3 levels. HDAC6 knockdown was confirmed by probing with HDAC6 antibody and α-Tubulin served as loading control. Bar graphs depict quantitative densitometry analysis of western blot experiments; n = 3; **p < 0.05. Data are expressed as mean ± SD. C - IL-6 levels in the EC conditioned medium after 6-h stimulation with PM were detected by ELISA assay. Data are presented as mean ± S.D.; n = 6, *p < 0.05.

pharmacological inhibitors of Rho GTPase and JAK signaling on EC permeability caused by PM and contractile agonist thrombin (Fig. 1E). Co-treatment with either a RhoA kinase inhibitor Y-27632 (2 μM), or a JAK kinase inhibitor (5 μM) significantly attenuated EC permeability induced by PM. Co-treatment with submaximal dose of thrombin (0.2 U/mL) further augmented EC barrier dysfunction caused by PM (20 μg/cm^2). The specificity and potency of inhibitors was verified by using known activators thrombin and IL-6 of Rho and JAK pathways, respectively. Detection of IL-6 levels in conditioned medium by ELISA assay showed that PM treatment stimulated the release of IL-6 in pulmonary EC in a concentration dependent fashion (Fig. 1F).

3.1. PM causes MT destabilization

Lately, there is a growing appreciation that MT dynamics plays a crucial role in the regulation of EC barrier [19]. Various EC barrier disruptive agonists, such as edemagenic agent thrombin or proinflammatory cytokine tumor necrosis factor-α (TNFα) cause MT destabilization, suggesting a key role of MT integrity during endothelial hyperpermeability and inflammation induced by these agonists [25,27]. We found that PM treatment of lung EC results in MT destabilization as evidenced by dissolution of peripheral MT network (Fig. 2A). Given that oxidant stress is involved in both PM-induced EC pathology as well as MT-mediated EC dysfunction [24,37,38], we tested whether PM destabilizes MT via ROS release.

To monitor PM-induced MT disassembly, we performed MT fractionation assay by isolating depolymerized and polymerized MT fractions as described in Methods. We observed a marked decrease in the pool of polymerized MT following PM treatment (Fig. 2A). A well-known MT destabilizer Nocadozole was used as a positive control. We also evaluated another parameter of MT stability, tubulin acetylation. EC treatment with PM dramatically reduced the network of acetylated MT as shown by immunofluorescence staining of EC with antibody to acetylated tubulin after 6 h of PM treatment (Fig. 2B). PM-induced decrease in acetylated tubulin levels was further confirmed by western blotting. PM reduced the acetylated tubulin immunoreactivity in a time-dependent manner (Fig. 2C). Arrangement of MT cytoskeleton in control and PM-challenged EC was further evaluated by immunofluorescence staining with α-tubulin antibody (Fig. 2D). Pretreatment of lung EC with ROS scavenger N-acetyl cysteine (NAC, 1 mM) suppressed the PM-induced MT disassembly. Protective effects of NAC against PM-induced MT disassembly were associated with NAC-induced suppression of the PM-induced decline of the pool of acetylated tubulin (Fig. 2E).

3.2. PM-caused EC barrier disruption is mediated by oxidative stress-induced HDAC6 activation

Because our results suggested a major role of MT in PM-induced EC dysfunction, we further investigated the cellular and molecular mechanisms involved in this process. HDAC6-mediated deacetylation of tubulin is a known mechanism of MT destabilization leading to endothelial barrier dysfunction [28,39,40]. Our results show that PM increased HDAC6 activity in pulmonary EC in a concentration-dependent manner (Fig. 3A). PM-induced elevation in HDAC6 activity was time dependent and consistent with development of PM-induced EC barrier

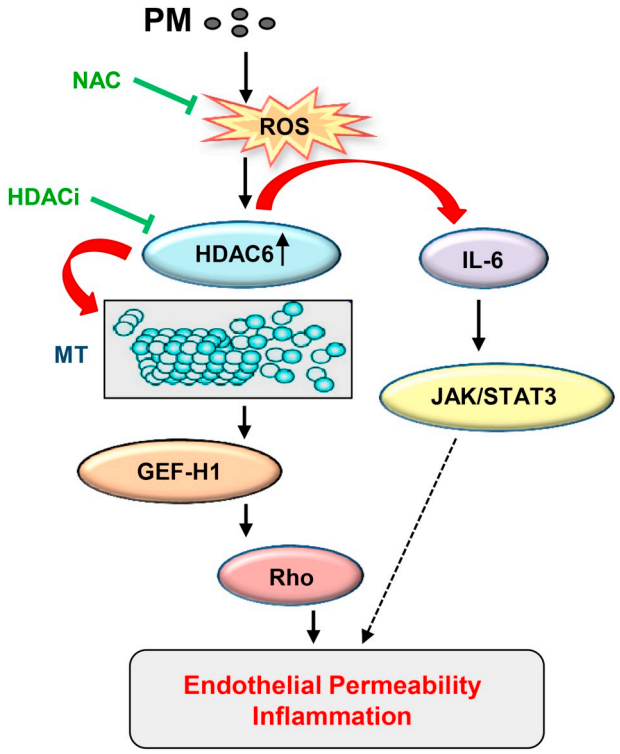

Fig. 6. Proposed mechanisms of PM-induced EC dysfunction via MT destabilization. PM induces ROS generation leading to oxidative HDAC6 activation which in turn destabilizes MT by deacetylation of a-tubulin within stable microtubules. MT depolymerization causes release of MT-bound GEF-H1 and subsequent activation of the Rho pathway. Simultaneously, PM-induced HDAC6 activation via positive feedback regulation of ROS production stimulates IL-6 expression and activation of JAK-STAT3 pathway of EC inflammation and barrier dysfunction. Both these signaling events ultimately result in increased EC permeability and inflammation.

dysfunction and was also dependent on oxidative stress, since the cell treatment with antioxidant NAC attenuated PM-induced HDAC6 activity at various time points (Fig. 3B). Next, we performed permeability assays to confirm the role of HDAC6 in PM-induced EC barrier disruption. Pretreatment with Tubastatin A (TubA), a pharmacological inhibitor specific to HDAC6, mitigated the TER drop in PM-challenged EC in a concentration-dependent manner, indicating improved barrier function (Fig. 3C). The efficacy of TubA to suppress HDAC6 activity was verified by western blot analysis of acetylated tubulin levels in total cell lysates from PM- and PM/TubA-treated EC (Inset, Fig. 3D). Immunofluorescence analysis of MT structure using staining with α-tubulin antibody showed that, as a result of HDAC6 inhibition, co-treatment of PM-challenged EC with TubA prevented PM-induced MT remodeling and preserved peripheral MT structure in the pulmonary EC (Fig. 3E).

MT disassembly stimulates actin stress fiber formation, EC contraction, and formation of the intercellular gaps via stimulation of the RhoA GTPase by its activator, RhoA-specific guanine nucleotide exchange factor GEF−H1, released from the microtubules [27,41]. Both NAC and TubA efficiently reduced PM-induced EC permeability for FITC-dextran tracer, strongly suggesting the involvement of ROS-HDAC6 signaling axis in MT destabilization and EC dysfunction caused by PM (Fig. 3F). In agreement with MT-dependent mechanism in PM-induced F-actin remodeling leading to EC barrier dysfunction, PM induced actin stress fibers and gap formation, which was attenuated by cell pretreatment with HDAC6 inhibitor (Fig. 3G).

3.3. Inhibition of HDAC6 attenuates PM-induced MT destabilization and suppresses Rho pathway

The studies from our group have illustrated that release of Rho activator GEF-H1 from destabilized MT induces EC permeability [42,43]. To investigate whether similar mechanism exists in PM-induced EC permeability via MT destabilization, we performed GEF-H1 pulldown assay by capturing active GEF-H1 bound to RhoG17A mutant protein beads. The data show that PM treatment activates GEF-H1 in pulmonary EC, and this effect is attenuated by the HDAC6 inhibitor TubA (Fig. 4A). Consistently, TubA inhibited PM-induced activation of Rho (Fig. 4B). We employed more direct approach of siRNA-mediated depletion of endogenous GEF-H1 in EC to test the role of GEF-H1 in exacerbation PM-induced EC permeability. Knockdown of GEF-H1 caused inhibition of PM-induced Rho activation and subsequent decrease in phospho-MLC levels (Fig. 4C and D). To further confirm that all of these aforementioned signaling pathways are involved in PM-induced EC dysfunction, we analyzed PM-enhanced phospho-MLC protein expression in the presence of inhibitors of oxidative stress, RhoA, or HDAC6. The results show a marked decrease in phospho-MLC levels in PM-challenged cells pretreated with ROS and HDAC6 inhibitors, and complete inhibition of MLC phosphorylation caused by Rho kinase inhibitor (Fig. 4E). SiRNA-induced knockdown of HDAC6 also decreased PM-induced MLC phosphorylation in pulmonary EC (Fig. 4F).

3.4. HDAC6 inhibition rescues PM-induced IL-6 production and STAT3 activation

We also examined the role of HDAC6 in PM-induced inflammatory signaling pathway mediated by IL-6 production and subsequent phosphorylation of STAT3. PM-caused increase in phospho-STAT3 levels was markedly decreased in the cells pretreated with antioxidant NAC and HDAC6 inhibitor TubA. Similarly, reduction of phospho-STAT3 to basal levels was achieved by the inhibition of JAK, an upstream activator of STAT3 (Fig. 5A). An essential contribution of HDAC6 in PM-caused induction of inflammatory signaling was further confirmed by experiments with siRNA-mediated knockdown of HDAC6, where PM failed to enhance STAT3 phosphorylation (Fig. 5B). Finally, genetic inhibition of HDAC6 significantly attenuated levels of IL-6 released into the culture medium by pulmonary EC challenged with PM (Fig. 5C).

4. Discussion

PM air pollution is continuously growing severe threat to human health globally, which ranks fifth among mortality risk factors [44]. A definite role of PM exposure in the development and progression of various cardiovascular, respiratory illnesses, and to some extent cerebrovascular diseases has now been well documented. ECs are vital for maintaining intact lung function, since increased EC permeability leads to a wide varieties of lung disorders including pulmonary edema, sepsis, acute lung injury (ALI) and acute respiratory distress syndrome (ARDS) [45,46]. A limited number of studies have suggested that ECs could be the vulnerable target of PM exposure, but precise mechanisms of PM-induced exacerbation of EC function remain largely unknown. In this study, we investigated the molecular mechanisms of PM-induced EC dysfunction. Our results revealed a novel role of MT dynamics regulated by oxidative stress-mediated activation of HDAC6. These data provide strong evidence that GEF-H1 release from destabilized MT and ensuing Rho activation is the key mechanism of PM-induced EC permeability. At the same time, PM-caused elevation of ROS levels leads to increased IL-6 production by EC, which also impairs EC barrier function via canonical JAK-STAT3 pathway (Fig. 6). To our knowledge, this is the first study to allocate the role of HDAC6-dependent MT regulation of EC barrier function in response to PM exposure.

The contribution of oxidative stress, Rho, and IL-6-dependent pathways in PM-induced EC dysfunction has been reported [16,17,47],

but the interplay between these signaling cascades and crucial mediators in the suggested mechanisms was lacking. The present study shows that PM is another inducer of ROS production and oxidant stress, and LPS and PM share the mechanism of EC barrier disruption via ROS-dependent depolymerization of MT. The current study provides the novel mechanistic information substantiating a central role of HDAC6 in PM-induced EC barrier failure via MT-dependent Rho activation. Increase in generation of ROS appears to be an initial step of PM-induced pathologic effects followed by stimulation of HDAC6 activity and deacetylation of tubulin leading to MT destabilization. HDAC6 is a unique deacetylase with cytosolic localization which targets tubulin and participates in regulation of MT dynamics. Recently, HDAC6 has gained attention with its new function in controlling vascular permeability [28,39,40].

We have previously demonstrated that activation of ROS production by bacterial lipopolysaccharide (LPS) decreased pools of polymerized actin, acetylated tubulin, and reduced the peripheral microtubule network. This effect was blocked by NAC [24]. PM exposure to EC in this study induced a rapid and sustained activation of HDAC6 that was dependent on redox signaling. The time frame of PM-induced early activation of HDAC6 is consistent with activation of GEF-H1-RhoA pathway and early increase in EC permeability. While we cannot exclude other mechanisms of PM-induced RhoA activation at early time points, our data strongly suggest a role for ROS-induced HDAC6 activation as an upstream event leading to activation of RhoA- and IL-6-mediated mechanisms of PM-induced EC barrier dysfunction (Figs. 2–5). We also acknowledge potential additional mechanisms driving the EC barrier failure beyond 24 h of PM exposure, which may involve activation of EC apoptosis, necroptosis, accelerated senescence, etc.

ROS scavenger NAC markedly reduced HDAC6 activity and also improved PM-caused EC barrier dysfunction to a similar degree with that of HDAC6 specific pharmacological inhibitor Tubastatin A (Fig. 3). Interestingly, our results also suggest an existence of positive feedback loop of ROS generation following HDAC6 activation and this additional ROS formation enhances IL-6 production by EC. This notion is supported by the results that both pharmacological and genetic inhibition of HDAC6 attenuates PM-induced IL-6 production and concomitant activation of STAT3 pathway (Fig. 5). These findings are also consistent with the previous study, which had shown upregulation of ROS production by HDAC6-induced stimulation of expression levels and enzymatic activity of NADPH oxidase, one of the key ROS-generating enzymes [48].

PM also activated Rho pathway of EC cytoskeletal remodeling and increased permeability. This study further advances our understanding of PM-induced activation of Rho signaling reported in recent study [16] and provides comprehensive evidence of PM-induced Rho activation via PM effects on MT dynamics. A consensus model of MT-mediated Rho activation resulting from studies by our and other groups is that release of MT-associated GEF-H1 activates Rho, which in turn, leads to formation of actin stress fibers and cell contraction causing endothelial permeability [42,49,50]. Our data suggest that MT-dependent activation of Rho pathway was preceded by ROS-mediated activation of HDAC6, which promoted MT disassembly. Both, the substantial loss of peripheral MT network and the decrease in the pool of acetylated MT caused by PM were prevented by cell treatment with antioxidants NAC and amifostine. The ablation of PM-induced Rho activation by inhibition of oxidative stress, HDAC6, or GEF-H1 clearly indicates a well-coordinated sequence of events that dictate PM actions on EC. Based on these findings, we propose a model whereby PM activates HDAC6 via ROS generation, and increased HDAC6 activity destabilizes MT with the release of GEF−H1, which activates Rho to ultimately cause alteration of EC cytoskeleton.

Our findings demonstrate that in parallel with MT-dependent Rho activation, PM activates IL-6 mediated canonical JAK-STAT3 pathway to cause EC dysfunction. Again, the increased IL-6 production by EC in response to PM treatment is facilitated by excessive ROS formation. A role of IL-6 in the development of PM-induced cardiopulmonary pathologies [5,6] and EC dysfunction [17] is well recognized. In addition, PM exposure enhances IL-6 expression in lung epithelial cells and macrophages [5,51], the cells which play essential roles in integral lung function, together with EC. These findings are highly consistent with an intriguing finding that PM causes the translocation of IL-6 from lung to the circulation, thereby inducing systemic inflammation [52]. In line with these reports, our findings highlight the crucial role of IL-6 mediated inflammatory pathways during PM-induced disorders. Our data provide novel information about PM-induced signaling events downstream of IL-6 and show that PM-induced JAK/STAT3 activation is not only blocked by antioxidants and JAK inhibitor, but it is also negatively regulated by inhibition of HDAC6. These findings suggest that activation of HDAC6 might serve as a crosstalk between MT-induced Rho activation and ROS-induced IL-6 production. Inhibition of ROS signaling prevented PM-induced IL-6 release [53]. Interestingly, IL-6 production by EC and other cell types may also be dependent on Rho activation [54,55]. These data suggest an additional positive feedback mechanism of RhoA and IL6 signaling amplification by PM [54,55].

5. Conclusion

In conclusion, this study describes a novel ROS/HDAC6-mediated, MT-associated signaling axis of PM-induced EC dysfunction. The proposed mechanism is summarized in Fig. 6. PM triggers several mechanisms (cytosolic and mitochondrial) leading to ROS production. HDAC6 is one of ROS targets; it becomes activated upon oxidation, which leads to deacetylation of a-tubulin, destabilization and partial disassembly of microtubules, and release of microtubule-bound Rho-specific GEF, GEF−H1. Upon release from MT, GEF-H1 becomes activated and stimulates Rho-MYPT-MLC mechanism of EC contractile response and permeability. Independently on MT regulation, activated HDAC6 also stimulates inflammatory cytokine IL-6 generation via positive feedback stimulation of ROS production, which sets an additional Jak/STAT3-dependent mechanism of EC inflammation and EC barrier disruption. Inhibition of PM-induced pathologic ROS production or suppression of HDAC6 activity mitigates PM-induced pulmonary EC permeability and inflammation. Thus, the dual role of HDAC6 in MT-dependent Rho activation as well as in ROS-mediated IL-6 production underscores the potential of HDAC6 inhibitors for the treatment of lung disorders associated with endothelial hyperpermeability and active inflammation. Considering the growing severity and adverse effects of PM air pollution on human health globally, identification of these crucial signaling pathways may aid in the development of effective therapeutics against PM-induced cardiopulmonary diseases.

Aknowledgements

This work was supported by the grants: HL107920, HL130431 from the National Heart, Lung, and Blood Institute, and GM114171 from the National Institute of General Medical Sciences.

References

[1] J. Lelieveld, J.S. Evans, M. Fnais, D. Giannadaki, A. Pozzer, Nature 525 (7569) (2015) 367–371.
[2] R.D. Brook, S. Rajagopalan, C.A. Pope 3rd, J.R. Brook, A. Bhatnagar, A.V. Diez-Roux, F. Holguin, Y. Hong, R.V. Luepker, M.A. Mittleman, A. Peters, D. Siscovick, S.C. Smith Jr., L. Whitsel, J.D. Kaufman, American heart association council on E, prevention CotKiCD, council on nutrition PA, Metabolism, Circulation 121 (21) (2010) 2331–2378.
[3] N.L. Mills, K. Donaldson, P.W. Hadoke, N.A. Boon, W. MacNee, F.R. Cassee, T. Sandstrom, A. Blomberg, D.E. Newby, Nat Clin Pract Cardiovasc Med 6 (1) (2009) 36–44.
[4] R. Sinharay, J. Gong, B. Barratt, P. Ohman-Strickland, S. Ernst, F.J. Kelly, J.J. Zhang, P. Collins, P. Cullinan, K.F. Chung, Lancet 391 (10118) (2018) 339–349.

[5] G.M. Mutlu, D. Green, A. Bellmeyer, C.M. Baker, Z. Burgess, N. Rajamannan, J.W. Christman, N. Foiles, D.W. Kamp, A.J. Ghio, N.S. Chandel, D.A. Dean, J.I. Sznajder, G.R. Budinger, J. Clin. Invest. 117 (10) (2007) 2952–2961.
[6] S.E. Chiarella, S. Soberanes, D. Urich, L. Morales-Nebreda, R. Nigdelioglu, D. Green, J.B. Young, A. Gonzalez, C. Rosario, A.V. Misharin, A.J. Ghio, R.G. Wunderink, H.K. Donnelly, K.A. Radigan, H. Perlman, N.S. Chandel, G.R. Budinger, G.M. Mutlu, J. Clin. Invest. 124 (7) (2014) 2935–2946.
[7] G.R. Budinger, J.L. McKell, D. Urich, N. Foiles, I. Weiss, S.E. Chiarella, A. Gonzalez, S. Soberanes, A.J. Ghio, R. Nigdelioglu, E.A. Mutlu, K.A. Radigan, D. Green, H.C. Kwaan, G.M. Mutlu, PLoS One 6 (4) (2011) e18525.
[8] S. Soberanes, D. Urich, C.M. Baker, Z. Burgess, S.E. Chiarella, E.L. Bell, A.J. Ghio, A. De Vizcaya-Ruiz, J. Liu, K.M. Ridge, D.W. Kamp, N.S. Chandel, P.T. Schumacker, G.M. Mutlu, G.R. Budinger, J. Biol. Chem. 284 (4) (2009) 2176–2186.
[9] T. Xia, M. Kovochich, A.E. Nel, Front. Biosci. 12 (2007) 1238–1246.
[10] A. Baccarelli, R.O. Wright, V. Bollati, L. Tarantini, A.A. Litonjua, H.H. Suh, A. Zanobetti, D. Sparrow, P.S. Vokonas, J. Schwartz, Am. J. Respir. Crit. Care Med. 179 (7) (2009) 572–578.
[11] V. Bollati, B. Marinelli, P. Apostoli, M. Bonzini, F. Nordio, M. Hoxha, V. Pegoraro, V. Motta, L. Tarantini, L. Cantone, J. Schwartz, P.A. Bertazzi, A. Baccarelli, Environ. Health Perspect. 118 (6) (2010) 763–768.
[12] L. Cantone, S. Iodice, L. Tarantini, B. Albetti, I. Restelli, L. Vigna, M. Bonzini, A.C. Pesatori, V. Bollati, Environ. Res. 152 (2017) 478–484.
[13] E. Tamagawa, N. Bai, K. Morimoto, C. Gray, T. Mui, K. Yatera, X. Zhang, L. Xing, Y. Li, I. Laher, D.D. Sin, S.F. Man, S.F. van Eeden, Am. J. Phys. Lung Cell. Mol. Phys. 295 (1) (2008) L79–L85.
[14] L. Calderon-Garciduenas, R. Villarreal-Calderon, G. Valencia-Salazar, C. Henriquez-Roldan, P. Gutierrez-Castrellon, R. Torres-Jardon, N. Osnaya-Brizuela, L. Romero, R. Torres-Jardon, A. Solt, W. Reed, Inhal. Toxicol. 20 (5) (2008) 499–506.
[15] Pope CA, 3rd, Bhatnagar A, McCracken JP, Abplanalp W, Conklin DJ, O'Toole T. Circ. Res. 2016;119(11):1204–1214.
[16] T. Wang, Y. Shimizu, X. Wu, G.T. Kelly, X. Xu, L. Wang, Z. Qian, Y. Chen, J.G.N. Garcia, Pulm. Circ. 7 (3) (2017) 617–623.
[17] J. Dai, C. Sun, Z. Yao, W. Chen, L. Yu, M. Long, FEBS Open Bio. 6 (7) (2016) 720–728.
[18] T.K. Akhshi, D. Wernike, A. Piekny, Cytoskeleton (Hoboken) 71 (1) (2014) 1–23.
[19] I.B. Alieva, E.A. Zemskov, K.M. Smurova, I.N. Kaverina, A.D. Verin, J. Cell. Biochem. 114 (10) (2013) 2258–2272.
[20] G. Piperno, M. Ledizet, X.J. Chang, J. Cell Biol. 104 (2) (1987) 289–302.
[21] E. Nogales, Annu. Rev. Biochem. 69 (2000) 277–302.
[22] A.A. Birukova, K. Smurova, K.G. Birukov, P. Usatyuk, F. Liu, K. Kaibuchi, A. Ricks-Cord, V. Natarajan, I. Alieva, J.G. Garcia, A.D. Verin, J. Cell. Physiol. 201 (1) (2004) 55–70.
[23] A.A. Birukova, K.G. Birukov, B. Gorshkov, F. Liu, J.G. Garcia, A.D. Verin, Am. J. Phys. Lung Cell. Mol. Phys. 289 (1) (2005) L75–L84.
[24] E. Kratzer, Y. Tian, N. Sarich, T. Wu, A. Meliton, A. Leff, A.A. Birukova, Am. J. Respir. Cell Mol. Biol. 47 (5) (2012) 688–697.
[25] I. Petrache, A. Birukova, S.I. Ramirez, J.G. Garcia, A.D. Verin, Am. J. Respir. Cell Mol. Biol. 28 (5) (2003) 574–581.
[26] A.D. Verin, A. Birukova, P. Wang, F. Liu, P. Becker, K. Birukov, J.G. Garcia, Am. J. Phys. Lung Cell. Mol. Phys. 281 (3) (2001) L565–L574.
[27] A.A. Birukova, K.G. Birukov, K. Smurova, D. Adyshev, K. Kaibuchi, I. Alieva, J.G. Garcia, A.D. Verin, FASEB J. 18 (15) (2004) 1879–1890.
[28] C. Hubbert, A. Guardiola, R. Shao, Y. Kawaguchi, A. Ito, A. Nixon, M. Yoshida, X.F. Wang, T.P. Yao, Nature 417 (6887) (2002) 455–458.
[29] Y. Zilberman, C. Ballestrem, L. Carramusa, R. Mazitschek, S. Khochbin, A. Bershadsky, J. Cell Sci. 122 (2009) 3531–3541 Pt 19.
[30] Y.S. Gao, C.C. Hubbert, J. Lu, Y.S. Lee, J.Y. Lee, T.P. Yao, Mol. Cell. Biol. 27 (24) (2007) 8637–8647.
[31] O. Dubrovskyi, A.A. Birukova, K.G. Birukov, Lab. Investig. 93 (2) (2013) 254–263.
[32] A.A. Birukova, D. Burdette, N. Moldobaeva, J. Xing, P. Fu, K.G. Birukov, Microvasc. Res. 79 (2) (2010) 128–138.
[33] V. Spindler, N. Schlegel, J. Waschke, Cardiovasc. Res. 87 (2) (2010) 243–253.
[34] K. Riento, A.J. Ridley, Nat. Rev. Mol. Cell Biol. 4 (6) (2003) 446–456.
[35] A.V. Villarino, Y. Kanno, J.R. Ferdinand, J.J. O'Shea, J. Immunol. 194 (1) (2015) 21–27.
[36] H. Gao, R.F. Guo, C.L. Speyer, J. Reuben, T.A. Neff, L.M. Hoesel, N.C. Riedemann, S.D. McClintock, J.V. Sarma, N. Van Rooijen, F.S. Zetoune, P.A. Ward, J. Immunol. 172 (12) (2004) 7703–7712.
[37] T. Xia, M. Kovochich, A. Nel, Clin. Occup. Environ. Med. 5 (4) (2006) 817–836.
[38] S.M. Craige, S. Kant, J.F. Keaney Jr., Circ. J. 79 (6) (2015) 1145–1155.
[39] D. Borgas, E. Chambers, J. Newton, J. Ko, S. Rivera, S. Rounds, Q. Lu, Am. J. Respir. Cell Mol. Biol. 54 (5) (2016) 683–696.
[40] J. Yu, Z. Ma, S. Shetty, M. Ma, J. Fu, Am. J. Phys. Lung Cell. Mol. Phys. 311 (1) (2016) L39–L47.
[41] A.D. Verin, A. Birukova, P. Wang, F. Liu, P. Becker, K. Birukov, J.G. Garcia, Am. J. Phys. Lung Cell. Mol. Phys. 281 (3) (2001) L565–L574.
[42] A.A. Birukova, D. Adyshev, B. Gorshkov, G.M. Bokoch, K.G. Birukov, A.D. Verin, Am. J. Phys. Lung Cell. Mol. Phys. 290 (3) (2006) L540–L548.
[43] X. Tian, Y. Tian, G. Gawlak, N. Sarich, T. Wu, A.A. Birukova, J. Biol. Chem. 289 (8) (2014) 5168–5183.
[44] Cohen AJ, Brauer M, Burnett R, Anderson HR, Frostad J, Estep K, Balakrishnan K, Brunekreef B, Dandona L, Dandona R, Feigin V, Freedman G, Hubbell B, Jobling A, Kan H, Knibbs L, Liu Y, Martin R, Morawska L, Pope CA, 3rd, Shin H, Straif K, Shaddick G, Thomas M, van Dingenen R, van Donkelaar A, Vos T, Murray CJL, Forouzanfar MH. Lancet 2017;389(10082):1907–1918.
[45] N.A. Maniatis, S.E. Orfanos, Curr. Opin. Crit. Care 14 (1) (2008) 22–30.
[46] K. Peters, R.E. Unger, J. Brunner, C.J. Kirkpatrick, Cardiovasc. Res. 60 (1) (2003) 49–57.
[47] T. Wang, E.T. Chiang, L. Moreno-Vinasco, G.D. Lang, S. Pendyala, J.M. Samet, A.S. Geyh, P.N. Breysse, S.N. Chillrud, V. Natarajan, J.G. Garcia, Am. J. Respir. Cell Mol. Biol. 42 (4) (2010) 442–449.
[48] G.S. Youn, K.W. Lee, S.Y. Choi, Park J. Free Radic, Biol. Med. 97 (2016) 14–23.
[49] Y.C. Chang, P. Nalbant, J. Birkenfeld, Z.F. Chang, G.M. Bokoch, Mol. Biol. Cell 19 (5) (2008) 2147–2153.
[50] M. Krendel, F.T. Zenke, G.M. Bokoch, Nat. Cell Biol. 4 (4) (2002) 294–301.
[51] J.L. Quay, W. Reed, J. Samet, R.B. Devlin, Am. J. Respir. Cell Mol. Biol. 19 (1) (1998) 98–106.
[52] T. Kido, E. Tamagawa, N. Bai, K. Suda, H.H. Yang, Y. Li, G. Chiang, K. Yatera, H. Mukae, D.D. Sin, S.F. Van Eeden, Am. J. Respir. Cell Mol. Biol. 44 (2) (2011) 197–204.
[53] J. Wang, J. Huang, L. Wang, C. Chen, D. Yang, M. Jin, C. Bai, Y. Song, J. Thorac. Dis. 9 (11) (2017) 4398–4412.
[54] S. Yamaguchi, K. Tanabe, S. Takai, R. Matsushima-Nishiwaki, S. Adachi, H. Iida, O. Kozawa, S. Dohi, Neurochem. Int. 55 (6) (2009) 438–445.
[55] P.Y. Mong, C. Petrulio, H.L. Kaufman, Q. Wang, J. Immunol. 180 (1) (2008) 550–558.